ISA Transactions 88 (2019) 23–36

Contents lists available at ScienceDirect

ISA Transactions

journal homepage: www.elsevier.com/locate/isatrans

Research article

Adaptive backstepping-based tracking control design for nonlinear active suspension system with parameter uncertainties and safety constraints

Hui Pang [a,*], Xu Zhang [a], Zeren Xu [b]

[a] School of Mechanical and Precision Instrument Engineering, Xi'an University of Technology, Xi'an, 710048, China
[b] International Center for Automotive Research (ICAR), Clemson University, Greenville, SC 29607, USA

HIGHLIGHTS

- A novel adaptive backstepping-based tracking controller is developed to stabilize motions of vehicle body and further to track the predefined reference trajectories within a finite time with achieving the improvements in riding comfort and handling stability of vehicle active suspension system.
- The stability analysis on zero dynamics system is conducted to ensure that all the safety performance indicators are all bounded and the corresponding upper bounds are estimable.

ARTICLE INFO

Article history:
Received 10 July 2018
Received in revised form 17 October 2018
Accepted 30 November 2018
Available online 6 December 2018

Keywords:
Active suspension system
Adaptive tracking control
Backstepping technique
Lyapunov stability theory

ABSTRACT

This paper proposes a novel constraint adaptive backstepping based tracking controller for nonlinear active suspension system with parameter uncertainties and safety constraints. By introducing the virtual control input and reference trajectories, the adaptive control law is developed to stabilize both of the vertical and pitch motions of vehicle body using backstepping technique and Lyapunov stability theory, and further to track the predefined reference trajectories within a finite time, which not only ensure the safety performance requirements, but also achieve improvements in riding comfort and handling stability of vehicle active suspension system. Next, the stability analysis on zero dynamics error system is conducted to ensure that all the safety performance indicators are all bounded and the corresponding upper bounds are estimable. Finally, a numerical simulation is provided to verify the effectiveness of the proposed controller and to address the comparability between the classical Barrier–Lyapunov Function based adaptive tracking controller and the proposed controller.

1. Introduction

Active suspension system is an effective way to isolate, absorb or dissipate the vibration energies transferred from the road surface disturbance to vehicle body, which can adjust itself and improve riding comfort and handling stability by ensuring the safety performance constraints of vehicle suspension system. When designing an active suspension system, it should satisfy such suspension performance requirements as (1) ride comfort, i.e., the minimization of vehicle body acceleration should be guaranteed, (2) the safety performance constraints including suspension dynamic displacement, tire dynamic load and actuator input saturation [1–3]. However, these performance requirements are usually conflicting, improving ride comfort will lead to a larger suspension work space, which usually imposes a great effect on chassis layout and then deteriorates vehicle handling stability and maneuverability. Therefore, it is necessary to manage the tradeoff between ride comfort and safety performance constraints for active suspension system.

Recently, a number of researchers have paid significant attention to the challenging issue of how to propose a reasonable control method to guarantee ride quality while providing handling stability as much as possible. Subsequently, many control strategies were proposed and reported in literatures [4–10] therein. Among these control schemes, the controller design was usually converted to a single objective control problem by characterizing ride comfort as the main control goal and the other safety performances as hard constraints in time domain. However, there unavoidably exist some uncertain parameters in active suspension system, such as vehicle body mass and its moment of inertia caused by the changeable number of passenger and dynamic loads. This will absolutely make it difficult to develop an accurate dynamic model and further to design an appropriate controller. Therefore, the adaptive backstepping technique has been extensively employed

* Corresponding author.
E-mail address: huipang@163.com (H. Pang).

https://doi.org/10.1016/j.isatra.2018.11.047
0019-0578/

in the controller design for the strict-output feedback systems with uncertain parameters due to such merits of anti-input saturation, interference suspension, accurate control, good robustness over the conventional control approaches [11–17]. For example, the authors in [11] suggested an intelligent adaptive backstepping control using a recurrent neural network to control the mover position of a magnetic levitation apparatus to compensate for the uncertainties of friction force. The authors in [12,13] investigated the control synthesis for a general class of strict feedback nonlinear systems, and presented the controller design by introducing a hysteretic quantize to avoid chattering by using backstepping technique. For a class of nonlinear systems with sampled and delayed measurements, an adaptive fuzzy backstepping control procedure was addressed through the combination of backstepping technique with the classic adaptive fuzzy control method [14]. For a double-rope winding hoisting system, a robust nonlinear adaptive backstepping controller combined with a nonlinear disturbance observer was proposed with considering the parameter uncertainties and external disturbances. Experimental studies have verified the excellent performance of the proposed controller [15]. In [16], the nonminimum phase problem for a flexible hypersonic vehicle was addressed to study the relationship between nonminimum phase and backstepping control and further to develop a stable nonlinear controller, which can guarantee the output tracking and internal stability well.

Motivated by the aforementioned studies, some scholars and researchers have carried out many remarkable researches in the control design for active suspension system. In [18,19], the adaptive controller was developed by a combination of selecting suitable Lyapunov function and non-linear backstepping control technique, which can deal with the parametric uncertainties, external disturbances and uncertain coefficients without control input in the hydraulic active suspension systems. Additionally, by linearizing the nonlinear suspension model based on H_∞ method, the authors in [20] developed an adaptive backstepping controller to guarantee the robustness of the closed-loop system in the presence of system uncertainties and to minimize the effect of road disturbance on the control system. An adaptive position control for a pump-controlled electrohydraulic actuator (EHA) was presented based on an adaptive backstepping control framework, and the core feature of this study was the combination of a modified backstepping algorithm with a special adaptation law to compensate for all nonlinearities and uncertainties in EHA system [21]. From the viewpoint of control method, although the above-mentioned control schemes have a low conservatism, nevertheless, less attention are paid to the safety performance constraints of suspension system. More specifically, the stability analysis on zero dynamics system is rarely discussed which often yields instability of the control system. Moreover, Barrier–Lyapunov Function (BLF) has been used by several researchers to deal with the nonlinear constraints [22–25] when developing an adaptive backstepping controller. It should be noted that the control principle of BLF method is choosing a specific Lyapunov candidate function with the property of growing to infinity if the function parameters are restrained within a certain limit, which ensures the satisfaction of the performance constraints for the closed-loop system and provides some inspirations for the follow-up studies.

On the other hand, Quadratic-Lyapunov Function (QLF) was also widely utilized in designing the adaptive backstepping controllers for vehicle suspension system. For instance, the authors in [26] conducted a comparative study of BLF and QLF based backstepping controllers for stabilizing the vertical displacement of a quarter-car active suspension system in dealing with the uncertain sprung mass, and the simulation result showed that the former backstepping controller has less conservatism while the later one has a higher accuracy in trajectory tracking. Similarly, the authors in [27] studied the adaptive backstepping control design based on BLF and QLF approach and proposed the backstepping controller to tolerate with the system uncertainties. A backstepping control design was proposed for a non-linear full vehicle suspension by using QLF-based adaptive feedback control law [28]. However, the model uncertainties were not taken into consideration, only the estimated equivalent control input was utilized to design the backstepping controller. To fulfill the coordination control over the vertical acceleration and suspension dynamic displacement, an intelligent fuzzy logic controller [29] was proposed based on QLF method, yet the tracking errors are not considered. Therefore, it is still a challenge to develop an adaptive backstepping-based tracking controller for nonlinear active suspension system with the parameter uncertainties and safety performance constraints.

Based on the above discussions, this paper proposes an enhanced adaptive backstepping-based tracking controller for nonlinear active suspension system with the system parameter uncertainties and safety performance constraints. To stabilize both of the vertical and pitch motions of vehicle body, the virtual control inputs and reference trajectories are introduced to establish the dynamic tracking system, and then an adaptive control law is designed to asymptotically track the predefined reference trajectories within a finite time and to satisfy the safety performance requirements in the presence of uncertain vehicle sprung-mass and its moment of inertia. Simultaneously, the stability analysis on zero dynamics system is conducted to ensure the boundness of the safety performance constraints. Finally, a numerical simulation case is provided to verify the proposed controller under bump, random and periodic road surface.

The rest of this paper is organized as follows: Section 2 presents system modeling of active suspension system and problem formulation. The proposed adaptive backstepping-based tracking control scheme is specifically discussed in Section 3. In Section 4, simulation investigation is presented to demonstrate the effectiveness and comparability of the designed controller. The conclusions are given in Section 5.

2. System modeling and problem formulation

A half-vehicle model is considered and shown in Fig. 1 with freedoms of motion in the heave and pitch directions, this model has been extensively used in the previous literatures [30,31] due to its symmetry. In this model, m_s and I_y denote the sprung mass and its moment of inertia, m_{uf} and m_{ur} denote the unsprung mass of the front and rear suspension, respectively; a and b denote the horizontal distances from the center of gravity (CG) of vehicle body to the front and rear axles, respectively; z_c and ϕ denote the vertical and angular displacement at the CG of vehicle body, respectively; z_{uf} and z_{ur} represent the vertical displacement of the front and rear unsprung masses, respectively; z_{rf} and z_{rr} represent the road disturbance inputs to the front and rear wheels, respectively. The nonlinear spring and damper force for the front and rear suspensions are denoted as F_{sf} and F_{sr}, F_{cf} and F_{cr}, respectively; u_{cf} and u_{cr} represent the active control forces of the front and rear suspension, respectively; k_{tf}, k_{tr} and c_{tf}, c_{tr} represent the stiffness coefficients and the damping coefficients of the front and rear tire, respectively.

According to Newton's second law, the dynamic equations for this half-vehicle model shown in Fig. 1 can be expressed as

$$\begin{cases} m_s\ddot{z}_c + F_{sf} + F_{cf} + F_{sr} + F_{cr} - u_c = 0 \\ I_y\ddot{\phi} + [a(F_{sf} + F_{cf}) - b(F_{sr} + F_{cr})] - u_{c\phi} = 0 \\ m_{uf}\ddot{z}_{uf} - F_{sf} - F_{cf} + k_{tf}(z_{uf} - z_{rf}) + c_{tf}(\dot{z}_{uf} - \dot{z}_{rf}) + u_{cf} = 0 \\ m_{ur}\ddot{z}_{ur} - F_{sr} - F_{cr} + k_{tr}(z_{ur} - z_{rr}) + c_{tr}(\dot{z}_{ur} - \dot{z}_{rr}) + u_{cr} = 0 \end{cases} \quad (1)$$

In terms of the different controllers used for active suspension system, the subscript letter c in u_c, $u_{c\phi}$, u_{cf}, and u_{cr} can be determined as B or Q, which stands for BLF or QLF based controllers.

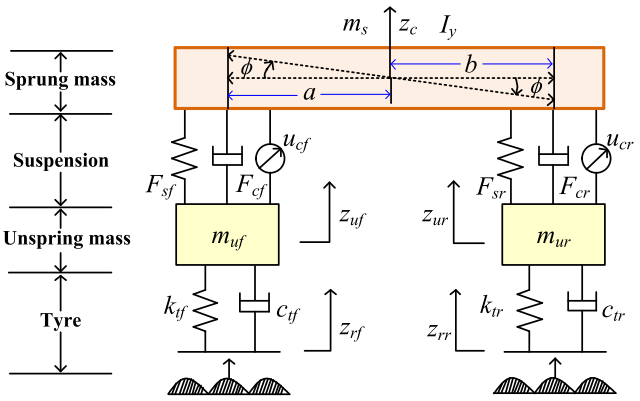

Fig. 1. Half-vehicle active suspension model.

Thus, in Eq. (1), the control forces of u_c and $u_{c\phi}$, are given by

$$\begin{aligned} u_c &= u_{cf} + u_{cr} \\ u_{c\phi} &= a u_{cf} - b u_{cr} \end{aligned} \tag{2}$$

In Eq. (1), F_{sf}, F_{sr}, F_{cf} and F_{cr} are given by [28]:

$$\begin{aligned} F_{sf} &= k_{sf}(z_c + a\sin\phi - z_{uf}) + k_{nsf}(z_c + a\sin\phi - z_{uf})^3 \\ F_{sr} &= k_{sr}(z_c - b\sin\phi - z_{ur}) + k_{nsr}(z_c - b\sin\phi - z_{uf})^3 \\ F_{cf} &= c_{sf}(\dot{z}_c + a\cos\phi\dot{\phi} - \dot{z}_{uf}) \\ F_{cr} &= c_{sr}(\dot{z}_c - b\cos\phi\dot{\phi} - \dot{z}_{ur}) \end{aligned} \tag{3}$$

where k_{sf} and k_{sr} , k_{nsf} and k_{nsr} are the stiffness coefficients of the linear and cubic terms, respectively; c_{sf} and c_{sr} represent the stiffness coefficients of the front and rear suspension, respectively, for simplicity, the suspension dynamic displacements of the front and rear suspension system are defined as follows:

$$\begin{cases} \Delta y_f = z_c + a\sin\phi - z_{uf} \\ \Delta y_r = z_c - b\sin\phi - z_{ur} \end{cases} \tag{4}$$

Next, define the state vector as $\boldsymbol{x} = [x_1, x_2, x_3, x_4, x_5, x_6, x_7, x_8]^T = [z_c, \dot{z}_c, \phi, \dot{\phi}, z_{uf}, \dot{z}_{uf}, z_{ur}, \dot{z}_{rr}]^T$, and then Eq. (1) can be rewritten as

$$\begin{cases} \dot{x}_1 = x_2 \\ \dot{x}_2 = \dfrac{1}{m_s}(-F_{sf} - F_{cf} - F_{sr} - F_{cr} + u_c) \\ \dot{x}_3 = x_4 \\ \dot{x}_4 = \dfrac{1}{I_y}(-a(F_{sf} + F_{cf}) + b(F_{sr} + F_{cr}) + u_{c\phi}) \\ \dot{x}_5 = x_6 \\ \dot{x}_6 = \dfrac{1}{m_{uf}}(F_{sf} + F_{cf} - k_{tf}(z_{uf} - z_{rf}) - c_{tf}(\dot{z}_{uf} - \dot{z}_{rf}) - u_{cf}) \\ \dot{x}_7 = x_8 \\ \dot{x}_8 = \dfrac{1}{m_{ur}}(F_{sr} + F_{cr} - k_{tr}(z_{ur} - z_{rr}) - c_{tr}(\dot{z}_{ur} - \dot{z}_{rr}) - u_{cr}) \end{cases} \tag{5}$$

In addition, due to the changeable number of passengers or dynamic payload, m_s and I_y will accordingly change in a certain range, so those two parameters are determined as the uncertain parameters of active suspension system. To facilitate the follow-up study, it is assumed that the known upper and lower bound of m_s and I_y satisfy

$$\begin{cases} m_s \in \{M: m_{s\min} \le m_s \le m_{s\max}\} \\ I_y \in \{I: I_{y\min} \le I_y \le I_{y\max}\} \end{cases} \tag{6}$$

To ensure that the controlled active suspension system has a better dynamic performance and satisfy the safety constraints, the following aspects should be considered [32] as:

(i) Ride comfort: The designed controller can guarantee the accurate trajectory tracking performances of the vertical and pitch displacement and then simultaneously achieve the minimization of the vertical acceleration and pitch angular acceleration.

(ii) Safety performance constraints

① Since it is needed to satisfy the limit of suspension mechanical structure, the suspension dynamic displacement should be restrained within its allowable maximum value, which is expressed by

$$\begin{cases} |\Delta y_f| \le \Delta y_{f\max} \\ |\Delta y_r| \le \Delta y_{r\max} \end{cases} \tag{7}$$

where $\Delta y_{f\max}$ and $\Delta y_{r\max}$ are the maximum suspension displacement limits for the front and rear suspension, respectively.

② To ensure vehicle riding safety, the dynamic loads of the front and rear tire should not exceed their static loads, which are given by

$$\begin{cases} F^f_{\text{ratio}} = \left|k_{tf}(z_{uf} - z_{rf}) + c_{tf}(\dot{z}_{uf} - \dot{z}_{rf})\right| / F_f < 1 \\ F^r_{\text{ratio}} = \left|k_{tr}(z_{ur} - z_{rr}) + c_{tr}(\dot{z}_{ur} - \dot{z}_{rr})\right| / F_r < 1 \end{cases} \tag{8}$$

where F^f_{ratio} and F^r_{ratio} denote the load ratio of the front and rear wheel, respectively; and the static loads of F_f and F_r are calculated by

$$\begin{cases} F_f + F_r = (m_s + m_{uf} + m_{ur})g \\ F_f(a+b) = m_s g a + m_f g(a+b) \end{cases} \tag{9}$$

In Eq. (9), the gravitational acceleration $g = 9.8\ \text{N/m}^2$.

③ The actuator input saturation should be taken into consideration in the controller design to satisfy the safety performance constraints of active suspension system. Here, the actuator control forces of the front and rear suspension should be smaller than their corresponding maximum limits $u_{cf\max}$ and $u_{cr\max}$, respectively, which is given by

$$\begin{cases} |u_{cf}| \le u_{cf\max} \\ |u_{cr}| \le u_{cr\max} \end{cases} \tag{10}$$

3. The adaptive backstepping controller synthesis

In this section, our main purpose is to develop the adaptive backstepping-based tracking controller for the closed-loop system in (5) by employing the backstepping technique and Lyapunov stability theory. This designed controller can ensure the asymptotic stability of the vertical and pitch motions of active suspension system when dealing with the uncertain parameters and external disturbances, and concurrently satisfy the safety performance constraints shown in Eqs. (7)–(10). To better illustrate the design procedure of the proposed controller, the classical BLF-based adaptive backstepping controller design are first introduced, and the desired QLF-based adaptive tracking controller is subsequently presented in detail. Note that the same initial constraints are imposed to both of the controllers in order to obtain the effective comparability.

3.1. The BLF-based controller design

The design process of the BLF-based adaptive backstepping controller is briefly presented in [33]. For system (5), define the tracking errors as $e_1 = x_1 - x_{1r}$, $e_3 = x_3 - x_{3r}$, $e_2 = x_2 - \beta_B$, $e_4 = x_4 - \beta_{1B}$, wherein x_{1r} and x_{3r} are respectively the reference trajectory, β_B and β_{1B} are respectively the virtual control function to be designed. We need to apply the BLF-based controller to make the tracking errors converge to zero asymptotically. In terms of the

boundness of the initial values for the BLF-based controller, the bounded Lyapunov candidate function is given as

$$V_{1B}(e_1) = \frac{1}{2}\ln\frac{\gamma_1^2}{\gamma_1^2 - {e_1}^2}$$
$$V_{3B}(e_3) = \frac{1}{2}\ln\frac{\gamma_3^2}{\gamma_3^2 - {e_3}^2} \tag{11}$$

where γ_1 and γ_3 are positive constant.

If β_B and β_{1B} are appropriately designed, the tracking errors of e_1 and e_3 will converge to zero within a preset time. To that end, the virtual control functions of β_B and β_{1B} are defined as follows:

$$\beta_B = \dot{x}_{1r} - k_1(\gamma_1^2 - {e_1}^2)e_1$$
$$\beta_{1B} = \dot{x}_{3r} - k_3(\gamma_3^2 - {e_3}^2)e_3 \tag{12}$$

where k_1 and k_3 are positive constants.

Taking the derivative of Eq. (11) gives

$$\dot{V}_{1B}(e_1) = \frac{e_1 e_2}{\gamma_1^2 - {e_1}^2} - k_1 e_1^2$$
$$\dot{V}_{3B}(e_3) = \frac{e_3 e_4}{\gamma_3^2 - {e_3}^2} - k_3 e_3^2 \tag{13}$$

In a similar way, the second bounded Lyapunov candidate functions are determined as

$$V_{2B} = V_{1B} + \frac{1}{2}e_2^2 + \frac{1}{2r_{\theta 1}}\widetilde{\theta}_1^2$$
$$V_{4B} = V_{3B} + \frac{1}{2}e_4^2 + \frac{1}{2r_{\theta 2}}\widetilde{\theta}_2^2 \tag{14}$$

where $\widetilde{\theta}_1 = \hat{\theta}_1 - \theta_1, \widetilde{\theta}_2 = \hat{\theta}_2 - \theta_2$ are respectively the differences between the estimated parameters of $\hat{\theta}_1, \hat{\theta}_2$ and the real value of θ_1, θ_2. Note that $\theta_1 \in [\theta_{1\min}, \theta_{1\max}], \theta_{1\min} = 1/m_{s\max}, \theta_{1\max} = 1/m_{s\min}$, $\theta_2 \in [\theta_{2\min}, \theta_{2\max}], \theta_{2\min} = 1/I_{y\max}, \theta_{2\max} = 1/I_{y\min}$.

To achieve the asymptotic stability of the vertical and pitch angular accelerations, the adaptive backstepping control law u_B and $u_{B\phi}$ are designed as

$$u_B = F_{cf} + F_{cr} + F_{sf} + F_{sr} + \frac{1}{\hat{\theta}_1}(\dot{\beta}_B - k_2 e_2 - \frac{e_1}{\gamma_1^2 - {e_1}^2})$$
$$u_{B\phi} = a(F_{cf} + F_{sf}) - b(F_{cr} + F_{sr}) + \frac{1}{\hat{\theta}_2}(\dot{\beta}_{1B} - k_4 e_4 - \frac{e_3}{\gamma_3^2 - {e_3}^2}) \tag{15}$$

where k_2 and k_4 are positive constants.

Following the projection adaptive laws in [34,35], the projection operator $proj_{\hat{\theta}_1}(r_{\theta_1} e_2 \tau_1(x,t))$ is given by

$$\dot{\hat{\theta}}_1(t) = proj_{\hat{\theta}_1}(r_{\theta_1} e_2 \tau_1(x,t)) = \begin{cases} 0, & \text{if } \hat{\theta}_1(t) = \theta_{1\max} \text{ and } r_{\theta_1} e_2 \tau_1(x,t) > 0 \\ 0, & \text{if } \hat{\theta}_1(t) = \theta_{1\min} \text{ and } r_{\theta_1} e_2 \tau_1(x,t) < 0 \\ r_{\theta_1} e_2 \tau_1(x,t), & \text{otherwise.} \end{cases} \tag{16}$$

where r_{θ_1} is a tunable positive value, and $\tau_1(x,t) = -F_{cf} - F_{cr} - F_{sf} - F_{sr} + u_B$.

Additionally, assuming that $\hat{\theta}_2$ is the estimated value of θ_2, and $\dot{\hat{\theta}}_2$ is then defined by

$$\dot{\hat{\theta}}_2(t) = proj_{\hat{\theta}_2}(r_{\theta_2} e_4 \tau_2(x,t)) = \begin{cases} 0, & \text{if } \hat{\theta}_2(t) = \theta_{2\max} \text{ and } r_{\theta_2} e_4 \tau_2(x,t) > 0 \\ 0, & \text{if } \hat{\theta}_2(t) = \theta_{2\min} \text{ and } r_{\theta_2} e_4 \tau_2(x,t) < 0 \\ r_{\theta_2} e_4 \tau_2(x,t), & \text{otherwise.} \end{cases} \tag{17}$$

where r_{θ_2} is a tunable positive value, and $\tau_2(x,t) = -a(F_{cf} + F_{sf}) + b(F_{cr} + F_{sr}) + u_{B\phi}$. It should be noticed that both of $\tau_1(x,t)$ and $\tau_2(x,t)$ are the force-related algebraic term.

Remark 1. It is known from Eq. (13) that $V_{1B}(e_1(0))$ is the maximum value of $V_{1B}(e_1)$ with $e_2 = 0$, thus only if the inequality $e_1(0) < \gamma_1$ holds, the constraint inequality $|e_1| < \gamma_1$ can be guaranteed in the entire time domain. Similarly, $V_{3B}(e_3(0))$ is the maximum value of $V_{3B}(e_3)$ with $e_4 = 0$, and only if $e_3(0) < \gamma_3$, the constraint inequality $|e_3| < \gamma_3$ can be guaranteed in the entire time domain.

The BLF-based adaptive backstepping controller design can be described as Theorem 1 [26].

Theorem 1. *By designing the adaptive laws expressed in (16) and (17), the adaptive control forces of (15) can be obtained with satisfying the following conditions:*

(1) The system (5) is asymptotically stable with $t \to \infty$, and all the output signals will gradually converge to zero;

(2) Only if the initial values of the vertical displacements at the CG of vehicle body are satisfied with $|x_1(0)| < \gamma_1$ and $|x_3(0)| < \gamma_2$, then $x_1(t)$ and $x_3(t)$ will definitely be restrained within the preset limits in the entire time domain.

(3) The safety performance requirements such as (7), (8) and (10) can be guaranteed.

3.2. The QLF-based controller design

To facilitate the proposed controller design, the following four design steps are used to fulfill the development of the adaptive QLF-based tracking controller. It is worth noting that the same expressions and symbols used in this section have the same definition as described in the BLF-based controller design.

Step 1. For the closed-loop system in (5), our main purpose is to develop an appropriate tracking controller to stabilize both of the vertical and pitch motions of vehicle body and make them accurately track the prescribed reference trajectories within a finite time, i.e. let the tracking errors of e_1 and e_3 converge to zero within a preset time. Then, taking the time derivative of e_1 and e_3 yields

$$\dot{e}_1 = x_2 - \dot{x}_{1r}, \dot{e}_3 = x_4 - \dot{x}_{3r} \tag{18}$$

To ensure that both of the proposed controller and the BLF-based controller have the same initial condition, it is required that $|x_1| < \gamma_1$ and $|x_3| < \gamma_3$ hold in the entire time domain. Moreover, define two virtual control functions as β_Q and β_{1Q} satisfying $x_2 = \beta_Q$ and $x_4 = \beta_{1Q}$, respectively.

If β_Q and β_{1Q} are viewed as the control inputs of e_2 and e_4, then both of e_2 and e_4 are redefined as

$$e_2 = x_2 - \beta_Q, e_4 = x_4 - \beta_{1Q} \tag{19}$$

It is obvious that (19) can be rewritten as

$$e_2 = \dot{x}_1 - \beta_Q, e_4 = \dot{x}_3 - \beta_{1Q} \tag{20}$$

Next, define two semi-definite Lyapunov candidate functions as

$$V_{1Q}(e_1) = \frac{1}{2}e_1^2, V_{3Q}(e_3) = \frac{1}{2}e_3^2 \tag{21}$$

Then, following the design of the virtual control functions of β_B and β_{1B}, we have

$$\beta_Q = \dot{x}_{1r} - k_1 e_1, \beta_{1Q} = \dot{x}_{3r} - k_3 e_3 \tag{22}$$

Differentiating (21) gives

$$\dot{V}_{1Q}(e_1) = e_1 e_2 - k_1 e_1^2, \dot{V}_{3Q}(e_3) = e_3 e_4 - k_3 e_3^2 \tag{23}$$

If the proposed controller has the desirable effect, which means $e_2 = 0$ and $e_4 = 0$, thus we have $\dot{V}_{1Q}(e_1) = -k_1 e_1^2 \le 0$ and $\dot{V}_{3Q}(e_3) = -k_3 e_3^2 \le 0$, and it is consequently easy to guarantee $e_1 \to 0$ and $e_3 \to 0$.

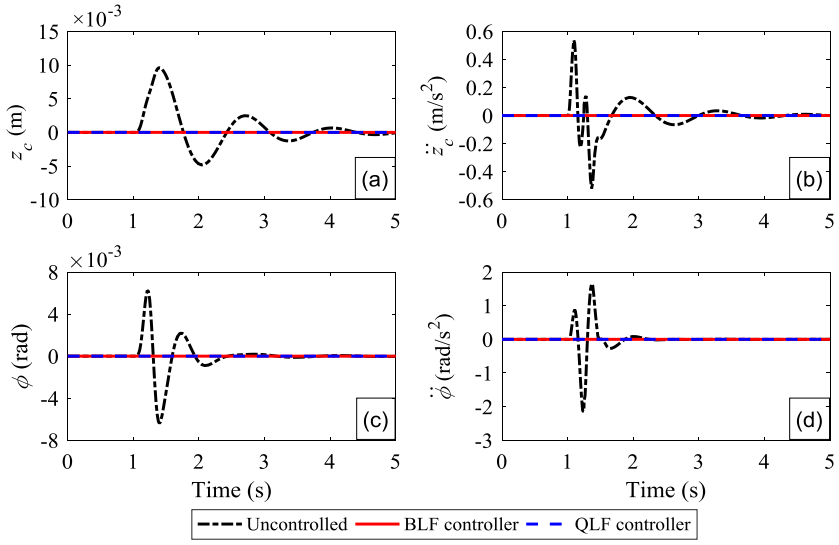

Fig. 2. Comparison of (a) vertical displacement, (b) vertical acceleration, (c) pitch angular and (d) pitch angular acceleration for active suspension system in Case I under bump road.

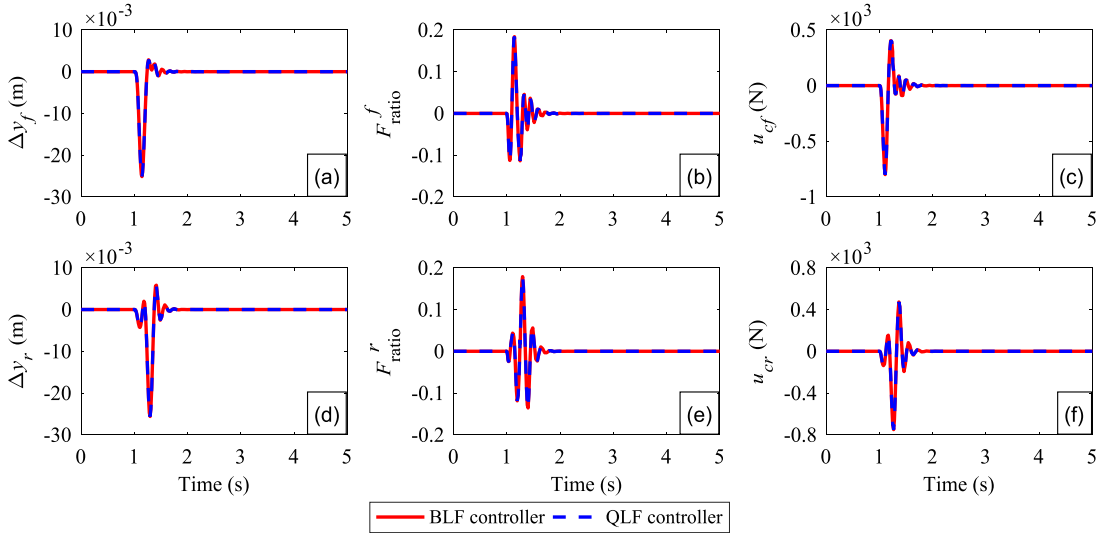

Fig. 3. Comparison of (a) suspension dynamic displacement of front wheel, (b) dynamic load ratio of front wheel, (c) initial control force of front wheel, (d) suspension dynamic displacement of rear wheel, (e) dynamic load ratio of rear wheel and (f) initial control force of rear wheel for active suspension system in Case I under bump road.

Step 2. Design the adaptive backstepping control law u_Q to make x_2 well track the designed virtual control input β_Q in the presence of the uncertain parameter θ_1 of m_s.

By taking the time derivative of e_2 in (19), one obtains

$$\dot{e}_2 = \theta_1 \tau_1(x,t) - \dot{\beta}_Q \tag{24}$$

where $\tau_1(x,t) = -F_{cf} - F_{cr} - F_{sf} - F_{sr} + u_Q$.

With the control objectives in mind, define u_Q as

$$u_Q = F_{cf} + F_{cr} + F_{sf} + F_{sr} + \frac{1}{\hat{\theta}_1}(\dot{\beta} - k_2(e_2) - e_1) \tag{25}$$

Select the same projection operator $\dot{\hat{\theta}}_{1Q}(t)$ as the BLF-based controller, which is given by

$$\dot{\hat{\theta}}_{1Q}(t) = proj_{\hat{\theta}_1}(r_{\theta_1} e_2 \tau_1(x,t)) \tag{26}$$

Then, define the second Lyapunov function $V_{2Q}(e_1, e_2, \widetilde{\theta}_1)$ as

$$V_{2Q}(e_1, e_2, \widetilde{\theta}_1) = \frac{1}{2}e_1^2 + \frac{1}{2}e_2^2 + \frac{1}{2}r_\theta^{-1}\widetilde{\theta}_1^2 \tag{27}$$

The time derivative of (27) is obtained as

$$\begin{aligned} \dot{V}_{2Q}(e_1, e_2, \widetilde{\theta}_1) &= -k_1 e_1^2 - k_2 e_2^2 + \widetilde{\theta}_1(r_{\hat{\theta}_1}^{-1}\dot{\hat{\theta}}_1 - e_2\tau_1(x,t)) \\ &\le -k_1 e_1^2 - k_2 e_2^2 \le 0 \end{aligned} \tag{28}$$

Integrating both sides of (28) from zero to arbitrary t yields

$$V_{2Q}(t) = \int_0^t \dot{V}_{2Q} d\tau + V_{2Q}(0) \le V_{2Q}(0) \tag{29}$$

According (27) to (29), it is observed that both of e_1 and e_2 are bounded, and $\widetilde{\theta}_1$ is also bounded. That is,

$$|e_1| \le \sqrt{2V_{2Q}(0)},\ |e_2| \le \sqrt{2V_{2Q}(0)} \tag{30}$$

From (30), we have

$$\begin{cases} |x_1| \le \|x_{1r}\|_\infty + \sqrt{2V_{2Q}(0)} \\ |x_2| \le \|\dot{x}_{1r}\|_\infty + (k_1+1)\sqrt{2V_{2Q}(0)} \end{cases} \tag{31}$$

It is equivalent to

$$-F_{sf} - F_{cf} - F_{sr} - F_{cr} + u_Q \in L_\infty \tag{32}$$

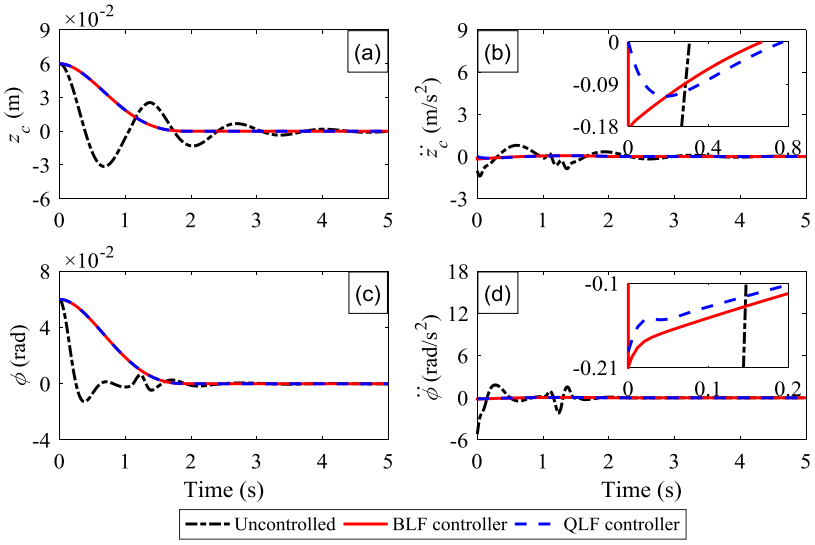

Fig. 4. Comparison of (a) vertical displacement, (b) vertical acceleration, (c) pitch angular and (d) pitch angular acceleration for active suspension system in Case II under bump road.

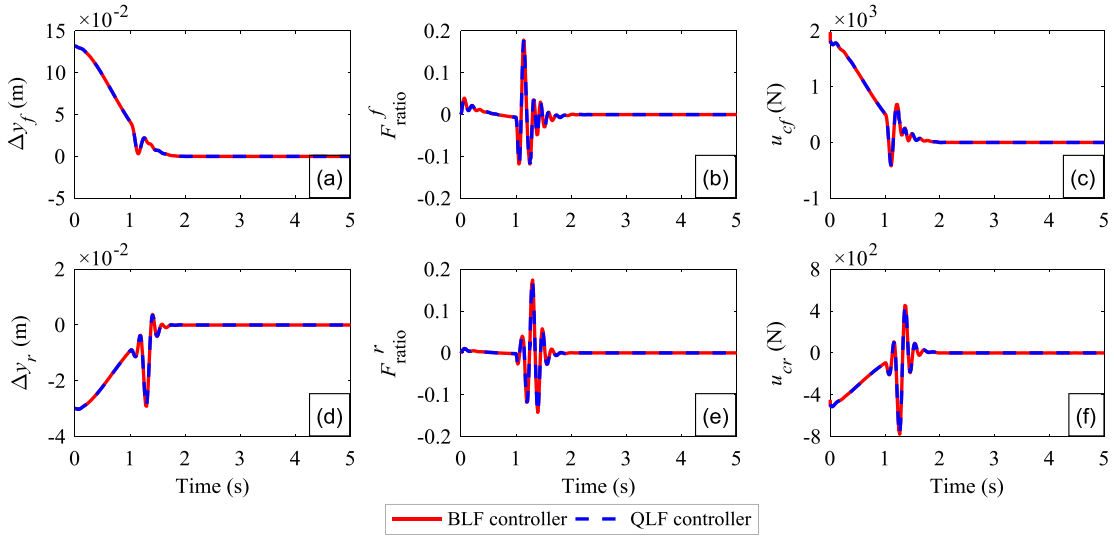

Fig. 5. Comparison of (a) suspension dynamic displacement of front wheel, (b) dynamic load ratio of front wheel, (c) initial control force of front wheel, (d) suspension dynamic displacement of rear wheel, (e) dynamic load ratio of rear wheel and (f) initial control force of rear wheel for active suspension system in Case II under bump road.

From (24) and (32), we obtain $\dot{e}_1$ and $\dot{e}_2 \in L_\infty$, and the derivative of (28) is obtained as

$$\ddot{V}_{2Q}(e_1, e_2, \widetilde{\theta}_1) \leq -2k_1e_1\dot{e}_1 - 2k_2e_2\dot{e}_2 \tag{33}$$

From (33), we have $\ddot{V}_{2Q} \in L_\infty$. Since $\dot{V}_2$ is uniformly continuous, based on Barbalat lemma and its proposition [36], we have $\dot{V}_{2Q} \to 0$ with $t \to \infty$. Therefore, we get $e_1 \to 0$ and $e_2 \to 0$, implying the tracking errors of e_1 and e_2 are asymptotically stable.

Step 3. Design the adaptive backstepping control law $u_{Q\phi}$ to make x_4 accurately track the designed virtual control input β_{1Q} in the presence of the uncertain parameter θ_2 of I_y. Noting that the design and proof procedure is similar to those in Step 2. For simplicity, the proof process of each sub-step is ignored and the corresponding design is directly presented as follows.

By taking the time derivative of e_4 in (20), one gets

$$\dot{e}_4 = \theta_2\tau_2(x, t) - \dot{\beta}_{1Q} \tag{34}$$

where $\tau_2(x, t) = -F_n + u_{Q\phi}$ and $F_n = a(F_{cf} + F_{sf}) - b(F_{cr} + F_{sr})$.

Choosing a specific Lyapunov candidate function as

$$V_{4Q} = \frac{1}{2}e_3^2 + \frac{1}{2}e_4^2 + \frac{1}{2r_{\theta_2}}\widetilde{\theta}_2^2 \tag{35}$$

It is noted that β_{1Q} has been defined in (22), then the adaptive backstepping function $u_{Q\phi}$ is herein selected as

$$u_{Q\phi} = F_n + \frac{1}{\hat{\theta}_2}(\dot{\beta}_1 - k_4(e_4) - e_3) \tag{36}$$

Define the projection operator $\dot{\hat{\theta}}_2$ as

$$\dot{\hat{\theta}}_2 = proj_{\hat{\theta}_2}(r_{\theta_2}e_4\tau_2(x, t)) \tag{37}$$

By conducting the same analysis as in Step 2, we conclude that e_3, e_4 and $\widetilde{\theta}_2$ are all bounded, that is,

$$\begin{cases} |x_3| \leq \|x_{3r}\|_\infty + \sqrt{2V_{4Q}(0)}, \\ |x_4| \leq \|\dot{x}_{3r}\|_\infty + (k_1 + 1)\sqrt{2V_{4Q}(0)}. \end{cases} \tag{38}$$

From the above analysis, we have $\dot{V}_{2Q} = -k_1e_1^2 - k_2e_2^2 \leq 0$ and $\dot{V}_{4Q} = -k_3e_3^2 - k_4e_4^2 \leq 0$, by further deriving, we can

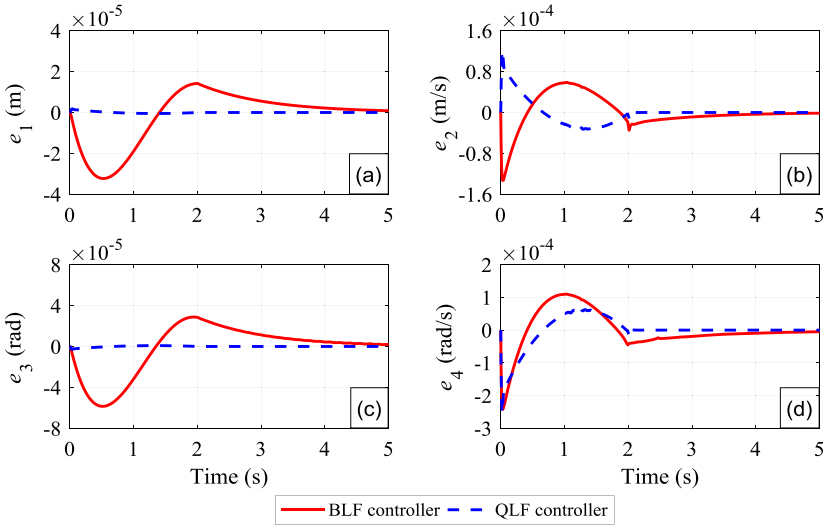

Fig. 6. Comparison of tracking errors for (a) vertical displacement, (b) vertical velocity, (c) pitch angular and (d) pitch angular velocity of active suspension system in Case II under bump road.

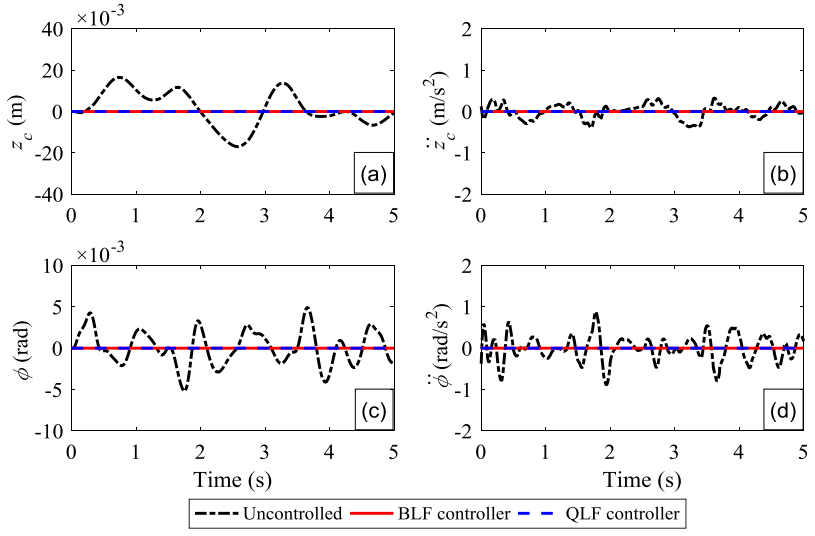

Fig. 7. Comparison of (a) vertical displacement, (b) vertical acceleration, (c) pitch angular and (d) pitch angular acceleration for active suspension system in Case I under random road.

obtain $V_{2Q}(t) \leq V_{2Q}(0)$ and $V_{4Q}(t) \leq V_{4Q}(0)$. If the trajectories of x_1 and x_3 satisfied the constraint conditions as $|x_1| \leq \gamma_1$ and $|x_3| \leq \gamma_3$, we can absolutely have $|x_{1r}(t)| + \sqrt{2V_{2Q}(0)} \leq \gamma_1$ and $|x_{3r}(t)| + \sqrt{2V_{4Q}(0)} \leq \gamma_3$. Therefore, when designing the reference trajectories, let the inequalities $|x_1| \leq \gamma_1$ and $|x_3| \leq \gamma_3$ hold, then we deservedly get $2V_{2Q}(0) < \gamma_1^2$ and $2V_{4Q}(0) < \gamma_3^2$. In other words, if the following inequalities

$$\begin{cases} e_1^2(0) + e_2^2(0) + \gamma_{\theta_1}^{-1}\tilde{\theta}_1^2 < \gamma_1^2 \\ e_3^2(0) + e_4^2(0) + \gamma_{\theta_2}^{-1}\tilde{\theta}_2^2 < \gamma_3^2 \end{cases} \tag{39}$$

hold, then $|x_1| \leq \gamma_1$ and $|x_3| \leq \gamma_3$ can be ensured.

Finally, it is concluded from (25) and (36) that the corresponding control force u_{Qf} and u_{Qr} are obtained as

$$\begin{cases} u_{Qf} = \dfrac{bu_Q + u_{Q\phi}}{a+b} \\ u_{Qr} = \dfrac{bu_Q - u_{Q\phi}}{a+b} \end{cases} \tag{40}$$

Step 4. To ensure the boundness and estimability of the safety constraint performances, it is extremely necessary to carry on the stability analysis of zero dynamics system. Since the adaptive backstepping design generates a four-order error dynamics system (e_1, e_2, e_3, e_4), while the original system (5) is an eight-order system, thus the zero dynamics system contains four states as x_5, x_6, x_7 and x_8. In order to find out them, one can set $x_1 = x_3 = 0$. Henceforth, we have

$$\begin{cases} u_Q = m_s\ddot{x}_{1r} + F_{sf} + F_{cf} + F_{sr} + F_{cr} \\ u_{Q\phi} = I_y\ddot{x}_{3r} + a(F_{sf} + F_{cf}) - b(F_{sr} + F_{cr}) \end{cases} \tag{41}$$

Substituting (41) into (5) gives the zero dynamics equation as

$$\dot{\mathbf{x}} = \mathbf{A}\mathbf{x} + \mathbf{B}\mathbf{z}_r + \mathbf{C}\mathbf{x}_r \tag{42}$$

where $\mathbf{x} = [x_5\ x_6\ x_7\ x_8]^T$, $\mathbf{z}_r = [z_{rf}\ \dot{z}_{rf}\ z_{rr}\ \dot{z}_{rr}]^T$ and $\mathbf{x}_r = [\ddot{x}_{1r}\ \ddot{x}_{3r}]^T$, and the corresponding coefficient matrices are as follows:

$$\mathbf{A} = \begin{bmatrix} 0 & 1 & 0 & 0 \\ -\dfrac{k_{tf}}{m_{uf}} & -\dfrac{c_{bf}}{m_{uf}} & 0 & 0 \\ 0 & 0 & 0 & 1 \\ 0 & 0 & -\dfrac{k_{tr}}{m_{ur}} & -\dfrac{c_{br}}{m_{ur}} \end{bmatrix},$$

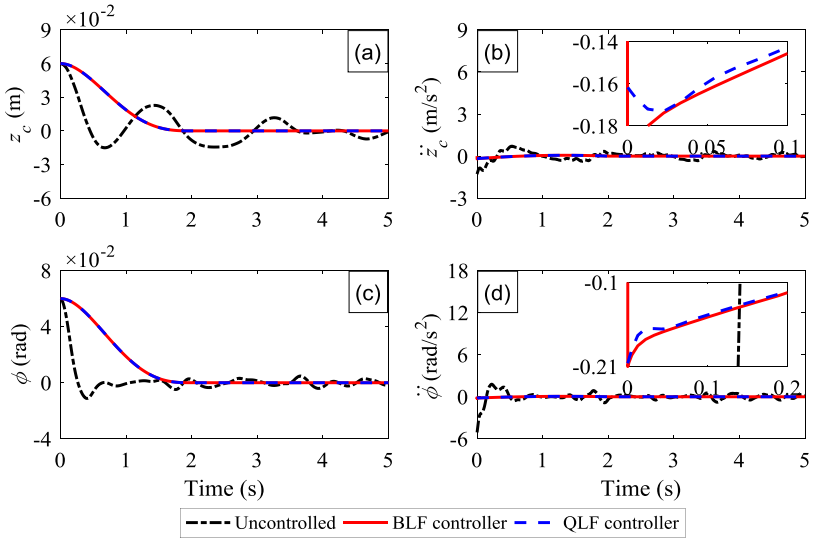

Fig. 8. Comparison of (a) vertical displacement, (b) vertical acceleration, (c) pitch angular and (d) pitch angular acceleration for active suspension system in Case II under random road.

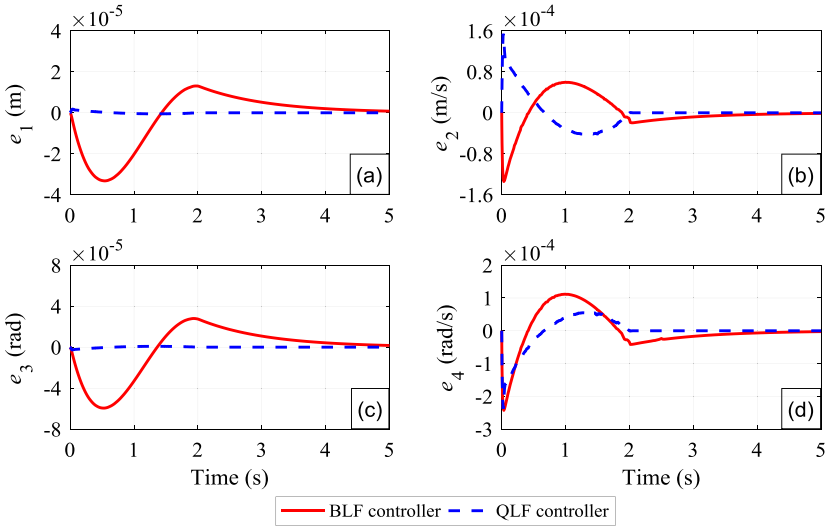

Fig. 9. Comparison of tracking errors for (a) vertical displacement, (b) vertical velocity, (c) pitch angular and (d) pitch angular velocity of active suspension system in Case II under random road.

$$\mathbf{B}=\begin{bmatrix} 0 & 0 & 0 & 0 \\ \frac{k_{tf}}{m_{uf}} & \frac{c_{bf}}{m_{uf}} & 0 & 0 \\ 0 & 0 & 0 & 0 \\ 0 & 0 & \frac{k_{tr}}{m_{ur}} & \frac{c_{br}}{m_{ur}} \end{bmatrix},$$

$$\mathbf{C}=\begin{bmatrix} 0 & 0 \\ -\frac{am_s}{m_{uf}(a+b)} & -\frac{I_y}{m_{uf}(a+b)} \\ 0 & 0 \\ \frac{bm_s}{m_{ur}(a+b)} & \frac{I_y}{m_{ur}(a+b)} \end{bmatrix}.$$

Define the positive definite function $V_{5Q}=\mathbf{x}^{\mathbf{T}}\mathbf{P}\mathbf{x}$ wherein $\mathbf{P}$ is a positive definite matrix, the derivative of V_{5Q} is given by

$$\dot{V}_{5Q}=\mathbf{x}^{\mathbf{T}}(\mathbf{A}^{\mathbf{T}}\mathbf{P}+\mathbf{P}\mathbf{A})\mathbf{x}+2\mathbf{x}^{\mathbf{T}}\mathbf{P}\mathbf{B}\mathbf{z}_r+2\mathbf{x}^{\mathbf{T}}\mathbf{P}\mathbf{C}\mathbf{x}_r \tag{43}$$

Because the real parts of the eigenvalue value for matrix $\mathbf{A}$ are all negative, we have $\mathbf{A}^{\mathbf{T}}\mathbf{P}+\mathbf{P}\mathbf{A}=-\mathbf{Q}$, wherein $\mathbf{Q}$ is a positive definite matrix [37]. Moreover, consider the following inequalities

$$\begin{cases} 2\mathbf{x}^{\mathbf{T}}\mathbf{P}\mathbf{B}\mathbf{z}_r \le \dfrac{1}{v_1}\mathbf{x}^{\mathbf{T}}\mathbf{P}\mathbf{B}\mathbf{B}^{\mathbf{T}}\mathbf{P}\mathbf{x}+v_1\mathbf{z}_r^{\mathbf{T}}\mathbf{z}_r \\ 2\mathbf{x}^{\mathbf{T}}\mathbf{P}\mathbf{C}\mathbf{x}_r \le \dfrac{1}{v_2}\mathbf{x}^{\mathbf{T}}\mathbf{P}\mathbf{C}\mathbf{C}^{\mathbf{T}}\mathbf{P}\mathbf{x}+v_2\mathbf{x}_r^{\mathbf{T}}\mathbf{x}_r \end{cases} \tag{44}$$

where v_1 and v_2 are tunable positive parameters. Based on (43) and (44), we obtain

$$\begin{aligned} \dot{V}_{5Q} &\le -\mathbf{x}^{\mathbf{T}}\mathbf{Q}\mathbf{x}+\frac{1}{v_1}\mathbf{x}^{\mathbf{T}}\mathbf{P}\mathbf{B}\mathbf{B}^{\mathbf{T}}\mathbf{P}\mathbf{x}+\frac{1}{v_2}\mathbf{x}^{\mathbf{T}}\mathbf{P}\mathbf{C}\mathbf{C}^{\mathbf{T}}\mathbf{P}\mathbf{x}+v_1\mathbf{z}_r^{\mathbf{T}}\mathbf{z}_r \\ &\quad +v_2\mathbf{x}_r^{\mathbf{T}}\mathbf{x}_r \\ &\le [-\lambda_{\min}(\mathbf{P}^{-\frac{1}{2}}\mathbf{Q}\mathbf{P}^{-\frac{1}{2}})+\frac{\lambda_{\max}}{v_1}(\mathbf{P}^{\frac{1}{2}}\mathbf{B}\mathbf{B}^{\mathbf{T}}\mathbf{P}^{\frac{1}{2}}) \\ &\quad +\frac{\lambda_{\max}}{v_2}(\mathbf{P}^{\frac{1}{2}}\mathbf{C}\mathbf{C}^{\mathbf{T}}\mathbf{P}^{\frac{1}{2}})]V_{5Q}+v_1\mathbf{z}_r^{\mathbf{T}}\mathbf{z}_r+v_2\mathbf{x}_r^{\mathbf{T}}\mathbf{x}_r \end{aligned} \tag{45}$$

Choosing matrix $\mathbf{P}$, $\mathbf{Q}$ with appropriate dimensions, as well as v_1 and v_2, the following (46) can be guaranteed as

$$\lambda_{\min}(\mathbf{P}^{-\frac{1}{2}}\mathbf{Q}\mathbf{P}^{-\frac{1}{2}})-\frac{\lambda_{\max}}{v_1}(\mathbf{P}^{\frac{1}{2}}\mathbf{B}\mathbf{B}^{\mathbf{T}}\mathbf{P}^{\frac{1}{2}})-\frac{\lambda_{\max}}{v_2}(\mathbf{P}^{\frac{1}{2}}\mathbf{C}\mathbf{C}^{\mathbf{T}}\mathbf{P}^{\frac{1}{2}})\ge\eta_1 \tag{46}$$

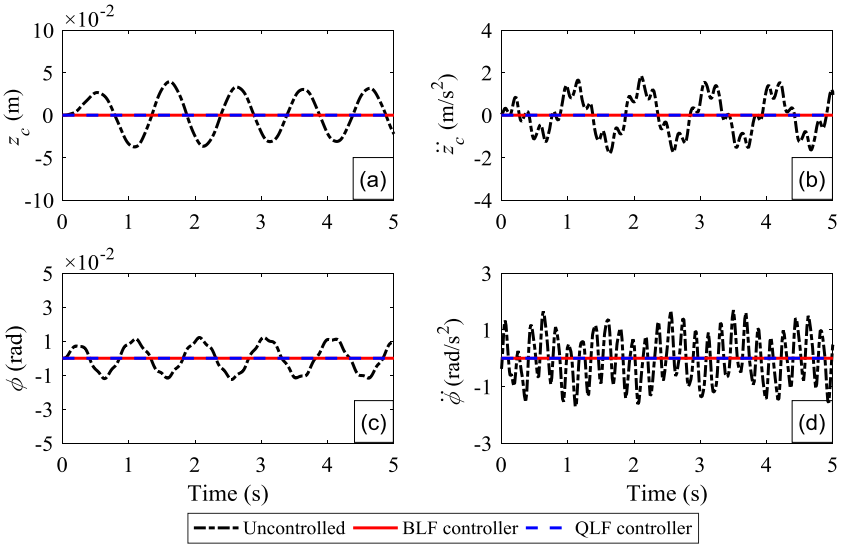

Fig. 10. Comparison of (a) vertical displacement, (b) vertical acceleration, (c) pitch angular and (d) pitch angular acceleration for active suspension system in Case I under periodic road.

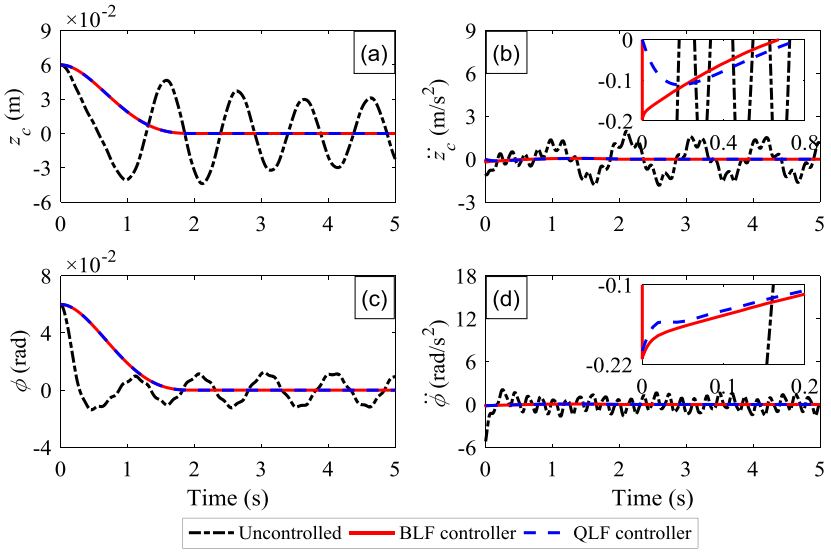

Fig. 11. Comparison of (a) vertical displacement, (b) vertical acceleration, (c) pitch angular and (d) pitch angular acceleration for active suspension system in Case II under periodic road.

where η_1 is a positive constant.

Define $\mathbf{z}_r^{\mathbf{T}}\mathbf{z}_r \leq \mathbf{z}_{r\max}$ and $\mathbf{x}_r^{\mathbf{T}}\mathbf{x}_r \leq \mathbf{x}_{r\max}$, and let $v_1\mathbf{z}_{r\max} + v_2\mathbf{x}_{r\max} = \eta_2$, thus we get

$$v_1\mathbf{z}_r^{\mathbf{T}}\mathbf{z}_r + v_2\mathbf{x}_r^{\mathbf{T}}\mathbf{x}_r \leq \eta_2 \tag{47}$$

where η_2 is a positive constant.

Further, we obtain $\dot{V}_{5Q} \leq -\eta_1 V_{5Q} + \eta_2$ and that $V_{5Q}(t)$ has the known boundness range, that is

$$V_{5Q}(t) \leq (V_{5Q}(0) - \frac{\eta_2}{\eta_1})e^{-\eta_1 t} + \frac{\eta_2}{\eta_1} = \varepsilon \tag{48}$$

Form (48), we have

$$|x_k| \leq \sqrt{\frac{\varepsilon}{\lambda_{\min}(\mathbf{P})}} \quad (k = 5, 6, 7, 8) \tag{49}$$

where

$$\varepsilon = \begin{cases} V_{5Q}(0), & \text{if } V_{5Q}(0) \geq \dfrac{\eta_2}{\eta_1} \\ \dfrac{2\eta_2}{\eta_1} - V_{5Q}(0), & \text{if } V_{5Q}(0) < \dfrac{\eta_2}{\eta_1} \end{cases}.$$

From the above-mentioned analysis, it is observed that all the signals are bounded within the known ranges, and the upper bound of suspension dynamic displacement can be estimated as

$$\begin{cases} |\Delta y_f| \leq \|x_1\|_\infty + a\|x_3\|_\infty + \frac{\sqrt{\varepsilon}}{\lambda_{\min}(\mathbf{P})} \\ \quad = \|x_{1r}\|_\infty + \sqrt{2V_{2Q}(0)} + a\|x_{3r}\|_\infty \\ \quad + a\sqrt{2V_{4Q}(0)} + \dfrac{\sqrt{\varepsilon}}{\lambda_{\min}(\mathbf{P})} = \Delta y_{fbd} \\ |\Delta y_r| \leq \|x_1\|_\infty + b\|x_3\|_\infty + \dfrac{\sqrt{\varepsilon}}{\lambda_{\min}(\mathbf{P})} \\ \quad = \|x_{1r}\|_\infty + \sqrt{2V_{2Q}(0)} + b\|x_{3r}\|_\infty \\ \quad + b\sqrt{2V_{4Q}(0)} + \dfrac{\sqrt{\varepsilon}}{\lambda_{\min}(\mathbf{P})} = \Delta y_{rbd} \end{cases} \tag{50}$$

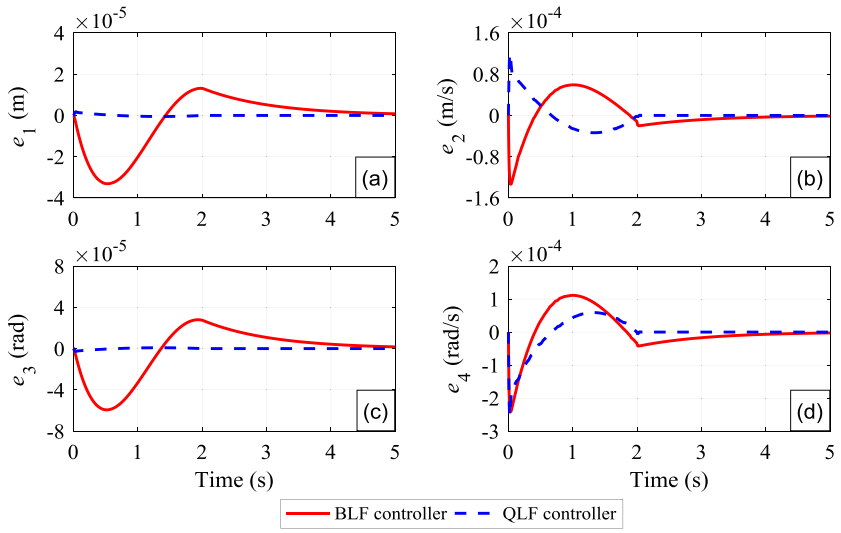

Fig. 12. Comparison of tracking errors for (a) vertical displacement, (b) vertical velocity, (c) pitch angular and (d) pitch angular velocity of active suspension system in Case II under periodic road.

Similarly, the upper bound of tire dynamic load is estimated as

$$\begin{cases} \left|F^f_{\text{ratio}}\right| = \left|k_{tf}(z_{uf}-z_{rf})+c_{tf}(\dot z_{uf}-\dot z_{rf})\right| \\ \quad \le \dfrac{(k_{tf}+c_{tf})\sqrt{\varepsilon}}{\lambda_{\min}(\mathbf{P})}+k_{tf}\left\|z_{rf}\right\|_\infty+c_{tf}\left\|\dot z_{rf}\right\|_\infty = F_{fbd} \\ \left|F^r_{\text{ratio}}\right| = \left|k_{tr}(z_{ur}-z_{rr})+c_{tr}(\dot z_{ur}-\dot z_{rr})\right| \\ \quad \le \dfrac{(k_{tf}+c_{tf})\sqrt{\varepsilon}}{\lambda_{\min}(\mathbf{P})}+k_{tr}\left\|z_{rr}\right\|_\infty+c_{tr}\left\|\dot z_{rr}\right\|_\infty = F_{rbd} \end{cases} \tag{51}$$

Further, the upper bound of actuator control input is estimated as

$$\begin{cases} \left|u_Q\right| \le \dfrac{1}{\theta_{1\min}}(\|\ddot x_{1r}\|_\infty+k_1\left|\dot e_1\right|+\left|e_1\right|+k_2\left|e_2\right|)+\left|F_{sf}\right| \\ \qquad +\left|F_{cf}\right|+\left|F_{sr}\right|+\left|F_{cr}\right| = u_{Qbd} \\ \left|u_{Q\phi}\right| \le \dfrac{1}{\theta_{2\min}}(\|\ddot x_{3r}\|_\infty+k_3\left|\dot e_3\right|+\left|e_3\right|+k_4\left|e_4\right|) \\ \qquad +a(\left|F_{sf}\right|+\left|F_{cf}\right|)+b(\left|F_{sr}\right|+\left|F_{cr}\right|) = u_{Q\phi bd} \end{cases} \tag{52}$$

The further derivation of (52) gives the upper bound of $\left|u_{Qf}\right|$ and $\left|u_{Qr}\right|$ as

$$\begin{cases} \left|u_{Qf}\right| = \dfrac{bu_{Qbd}+u_{Q\phi bd}}{a+b} = \left|u_{Qfbd}\right| \\ \left|u_{Qr}\right| = \dfrac{bu_{Qbd}+u_{Q\phi bd}}{a+b} = \left|u_{Qrbd}\right| \end{cases} \tag{53}$$

It is obvious that the following inequalities will hold through setting the system initial values and adjusting v_1 and v_2, in subsequent, the safety constraint performances shown in (7), (8) and (10) can all be guaranteed. That is,

$$\begin{cases} \left|\Delta y_f\right| \le \Delta y_{fbd} \le \Delta y_{f\max} \\ \left|\Delta y_r\right| \le \Delta y_{rbd} \le \Delta y_{r\max} \end{cases} \tag{54}$$

$$\begin{cases} \left|F^f_{\text{ratio}}\right| \le F_{fbd} \le F_f \\ \left|F^r_{\text{ratio}}\right| \le F_{rbd} \le F_r \end{cases} \tag{55}$$

$$\begin{cases} \left|u_{Qf}\right| \le u_{Qfbd} \le u_{Qf\max} \\ \left|u_{Qr}\right| \le u_{Qrbd} \le u_{Qr\max} \end{cases} \tag{56}$$

Based on the above discussion, the proposed QLF-based controller and its stability analysis can be summarized as Theorem 2 and Remark 2.

Theorem 2. *Considering the nonlinear active suspension system (5), the implementation of the designed control laws in (26) and (37) can ensure the following safety performance constraints such that*

(1) The closed-loop system (5) is asymptotically stable, i.e., all the output signals gradually converge to zero with $t\to\infty$.

(2) Only if the initial values of the vertical and pitch angular displacement z_c and ϕ are satisfied with the constraint condition in (39), then both of z_c and ϕ will be restrained within the preset limits in the entire time domain.

(3) Only if the initial values of system (5) satisfy the constraint conditions in (54)–(56), the suspension performance constraints as given in (7), (8) and (10) can be guaranteed.

Remark 2. From the above analysis, if the constraint conditions such as $|x_1| < \gamma_1$ and $|x_3| < \gamma_3$ hold, then the safety performance indicators shown in (7), (8) and (10) for active suspension system (5) can be ensured. In order to obtain $|x_1| < \gamma_1$ and $|x_3| < \gamma_3$, the initial values of safety performance constraints should be imposed on both of the QLF-based and BLF-based adaptive backstepping controllers with satisfying

$$\begin{cases} \text{QLF}: \ e_1^2(0)+e_2^2(0)+\gamma_{\theta1}^{-1}\widetilde\theta_1^2 < \gamma_1^2 \Rightarrow |x_1| < \gamma_1 \\ \text{QLF}: \ e_3^2(0)+e_4^2(0)+\gamma_{\theta2}^{-1}\widetilde\theta_2^2 < \gamma_3^2 \Rightarrow |x_3| < \gamma_3 \\ \text{BLF}: \ |e_1(0)| < \gamma_1 \Rightarrow |x_1| < \gamma_1 \\ \text{BLF}: \ |e_3(0)| < \gamma_1 \Rightarrow |x_3| < \gamma_3 \end{cases} \tag{57}$$

Actually, if tracking errors of $e_2(0)$ and $e_4(0)$, the estimated errors of $\widetilde\theta_1(0)$ and $\widetilde\theta_2(0)$ are equal to zero, both of the two controllers will satisfy the suspension displacement constraints whether the reference trajectories are introduced or not. However, the key point of the controller design is how to select such parameters as the initial values of the system state and controller gain, which is extremely crucial to guarantee the safety performance requirements. Therefore, the suspension safety performance can be guaranteed if the initial conditions for system (5) satisfy with the inequalities of (54)–(56).

3.3. The initial condition and reference trajectory

To verify the effectiveness of the proposed controller, consider the two cases with different initial values, wherein case I and case II are set as follows:

Case I: The initial values are $x_1(0) = 0$ cm, $x_3(0) = 0$ rad, $x_i = 0$, $i = 2, 4 \ldots 8$, $\theta_1(0) = 1/1100$, $\theta_2(0) = 1/550$, named as zero initial

Table 1
Model parameters of half-vehicle active suspension system.

M_s	I_y	m_{uf}	m_{ur}	a
1200 kg	600 kg m^2	100 kg	100 kg	1.2 m
b	k_{sr}	k_{sf}	k_{tr}	k_{tf}
1.5 m	15 000 N m^{-1}	15 000 N m^{-1}	200 000 N m^{-1}	150 000 N m^{-1}
c_{bf}	c_{br}	c_{sf}	c_{sf}	k_{nsf}, k_{nsr}
1500 N s m^{-1}	2000 N s m^{-1}	1500 N s m^{-1}	1200 N s m^{-1}	1000 N m^{-3}

condition; moreover the reference trajectory is set as $x_{1r} = 0$ and $x_{3r} = 0$. It should be noted that this study dedicates to minimize $z_c(t)$ and $\phi(t)$ under the external road disturbance, and to make the two performances indicators converge to zero asymptotically.

Case II: The initial values are $x_1(0) = 6$ cm, $x_3(0) = 6$ rad, $x_i = 0$, $i = 2, 4, \ldots, 8$, $\theta_1(0) = 1/1100$, $\theta_2(0) = 1/550$, named as non-zero initial condition. Additionally, we need to define a specific polynomial x_{ur} as the reference trajectory. It is worth pointing out that x_{ur} is a continuous derivable function satisfying $x_1 < \gamma_1$ and $x_3 < \gamma_3$. The designer can adjust $z_c(t)$ and $\phi(t)$ to reach a higher or lower level via setting different preset time t, which can further improve the ride quality of vehicle suspension system. The reference trajectory x_{ur} is defined as

$$x_{ur}(t) = \begin{cases} a_{u0} + a_{u1}t + a_{u2}t^2 + a_{u3}t^3 + a_{u4}t^4, & t < T_{ur} \\ 0, & t \geq T_{ur} \end{cases} \tag{58}$$

where the polynomial coefficients $a_{ui}(i = 0, 1, 2, 3, 4; u = 1, 3)$ are all constants, and are expressed by

$$\begin{aligned} &x_{ur}(0) = a_0 = x_1(0) \\ &\dot{x}_{ur}(0) = a_1 = x_2(0) \\ &x_{ur}(T_{ur}) = a_0 + a_1T_{ur} + a_2{T_{ur}}^2 + a_3{T_{ur}}^3 + a_4{T_{ur}}^4 = 0 \\ &\dot{x}_{ur}(T_{ur}) = a_1 + 2a_2T_{ur} + 3a_3{T_{ur}}^2 + 4a_4{T_{ur}}^3 = 0 \\ &\ddot{x}_{ur}(T_{ur}) = 2a_2 + 6a_3T_{ur} + 12a_4{T_{ur}}^2 = 0 \end{aligned} \tag{59}$$

The aforementioned (58) and (59) can ensure that the following conditions hold:

(1) The initial values of tracking errors of e_1 and e_3, and their first-order derivative are zero, i.e. $e_1(0) = \dot{e}_1(0) = 0, e_3(0) = \dot{e}_3(0) = 0$;

(2) The reference trajectory $x_{ur}(t)$ is second-order differentiable, i.e., $x_{ur}(t) \in C^2$. Theoretically, one can choose an arbitrary prescribed timeT_{ur}, and both of the vertical and pitch vibrations caused by the external disturbances will reach attenuation more quickly with a smaller T_{ur}. To this end, the reference trajectory with a decreasing polynomial form is selected to replace the zero reference curve, and set $T_{ur} = 2$ s.

4. Simulation investigation and discussion

A numerical simulation example is provided to demonstrate the effectiveness of the proposed controller under bump, random and periodic road excitation in Case I and Case II situations. The half-vehicle model parameters are listed in Table 1 and the designed parameters for the proposed controller are given as $r_{\theta 1} = r_{\theta 2} = 0.001$, $k_1 = k_2 = k_3 = k_4 = 100$, $\gamma_1 = \gamma_3 = 0.08$,$\theta_{1\min} = 1/1300$ kg, $\theta_{1\max} = 1/1000$ kg, $\theta_{2\min} = 1/700$ kg m^2, $\theta_{2\max} = 1/500$ kg m^2. The vehicle performances of Uncontrolled, the BLF-based backstepping controller and the proposed QLF-based backstepping controller are compared in this simulation.

For the controller design, it should be satisfied with the following four requirements

(1) The suspension vertical and pitch angular displacements are converged to zero within a preset time T_{ur}, i.e., $z_c \to 0$ and $\phi \to 0$ within T_{ur}.

(2) The front and rear suspension dynamic travels of Δy_f and Δy_r are less than the maximal value of suspension dynamic displacement $z_{\max} = 0.15$ m.

(3) The load ratios of the front and rear wheels represented by F^f_{ratio} and F^r_{ratio} should be less than one.

(4) The actuator control force of the front and rear wheels represented by u_{cf} and u_{cr} should satisfy the saturation limitation. Noting that the maximal value of control force is $u_{c\max} = 5000$ N.

4.1. Bump response

Generally, bump road excitation is employed to mimic an isolated shock on a smooth road surface [38], which is expressed as

$$z_{rf} = \begin{cases} \dfrac{h_b}{2}(1 - \cos(8\pi t)), & 1 \leq t \leq 1.25 \\ 0, & \text{otherwise} \end{cases} \tag{60}$$

where $h_b = 0.0\,2$ m is the height of road bump, $V = 45$ km/h is the vehicle forward velocity. Although the front and rear wheel have the same road input excitation, yet there exists a time delay of (a + b)/V.

4.1.1. Simulation analysis in Case I

Fig. 2 shows the time response comparison of the vertical displacement and acceleration, the pitch angular displacement and acceleration for active suspension system in Case I under bump road. It is observed from Fig. 2(a) and (c) that, compared to uncontrolled suspension system, the BLF-based and QLF-based controller can effectively isolate perturbations in the presence of the uncertain parameters and external road disturbance. From Fig. 2(b) and (d), it is seen that both of the two controllers can obviously improve the vertical and pitch angular acceleration, and the stability of vehicle dynamics performance can be achieved in a short time. It should be noted that both of the two controllers have almost the same control effect in Case I, implying that the two controllers have the same conservatism under zero initial condition.

Moreover, it can be seen from Fig. 3(a) and (d) that both of Δy_f and Δy_r are less than $z_{\max}$; by analyzing Fig. 3(b) and (e), we can obtain that F^f_{ratio} and F^r_{ratio} are always less than one, illustrating that the dynamic load is less than its static load and ensuring the firm uninterrupted contact of wheels to road. In addition to this, from Fig. 3(c) and (f), we can see that u_{cf} and u_{cr} are always less than the maximal control force $u_{c\max}$. Based on the above analysis, we can arrive at the conclusion that although there exists a significant shock for active suspension system when running across the bump road surface, both of the two controllers can guarantee the safety performance constraints for active suspension system under Case I condition.

4.1.2. Simulation analysis in Case II

In this case, we provide Figs. 4 and 5 to reveal the comparability of active suspension performance between uncontrolled, the BLF-based controller and the proposed QLF-based controller. As shown in Fig. 4(a) and (c), both of the latter two controllers can absorb the vibration energies generated by the external road disturbances. Simultaneously, it is seen from Fig. 4(b) and (d) that the vertical and pitch angular acceleration can be improved significantly for active suspension system with the BLF-based and QLF-based controllers, while the QLF-based controller has a smaller peak value of the vertical and pitch angular acceleration.

On the other hand, it is seen from Fig. 5(a) and (d) that the suspension dynamic displacements of active suspension system with the BLF-based and QLF-based controllers are always less $z_{\max}$. By analyzing the left sub-plots in Fig. 5, we can obtain that, the tire load ratios and actuator forces of these two controllers can meet

the performance requirements of active suspension system. In summary, regardless of how to choose the initial values, both of the two controllers can guarantee the suspension safety performance constraints under bump road excitation.

In order to further evaluate the designed controller, Fig. 6 gives the tracking errors of active suspension system with the two controllers in Case II under bump road excitation. It is clear that the tracking errors of the QLF-based controller can converge to zero in a shorter finite time for tracking the vertical displacement and velocity, the pitch angular displacement and velocity, respectively, which implies that the proposed controller has a better tracking performance.

4.2. Random response

The road excitation can also be generally assumed as random vibration that is consistent and typically specified as a white noise process given by [31]

$$G_q(n) = G_q(n_0)\,(n/n_0)^{-c} \tag{61}$$

where n is the spatial frequency and n_0 is the reference spatial frequency with $n_0 = 0.1(1/\mathrm{m})$, $G_q(n_0)$ is the road roughness coefficient; $c = 2$ is the road roughness constant. Combining the spatial frequency n with time frequency f, we have $f = nV$, where V is the vehicle forward velocity. For this simulation, we choose $G_q(n_0) = 64 \times 10^{-6}\ \mathrm{m}^3$ as C-class road, and the vehicle forward velocity $V = 72$ (km/h).

It is noted that the simulation curves of active suspension performances under random road surface are almost the same as the corresponding ones under bump road surface, which implies that both of the two controllers can well satisfy the suspension performance requirements when running on random road. To reduce redundancy in paragraph and reveal the prominent superiority of the proposed controller in tracking trajectory, we only provide the comparison of the vertical displacement and acceleration for active suspension system with the two different controllers under random road excitation in Case I and Case II situations, as well as the comparison of tracking errors under non-zero initial condition.

4.2.1. Simulation analysis in Case I

The comparison of time-domain response for the vertical displacement and acceleration, the pitch angular displacement and acceleration of active suspension system with these two controllers in Case I is presented in Fig. 7. It is worth pointing out that, according to Fig. 7(a) and (c), both of the BLF-based and QLF-based controllers can effectively isolate perturbations in the presence of random road disturbance compared to uncontrolled suspension system. Additionally, it is obviously seen from Fig. 7(b) and (d) that both of the two controllers can significantly improve the vertical and pitch angular accelerations to make the control system converge to a relatively stable state in less time.

4.2.2. Simulation analysis in Case II

The simulation result in Fig. 8 reveals the comparison of time-domain response for the vertical displacement and acceleration, the pitch angular displacement and acceleration of active suspension system with the two controllers under Case II condition.

As can be seen from Fig. 8(a) and (c), compared to uncontrolled suspension system, both of the two controllers can absorb the vibration energies generated by random road disturbance, moreover, according to Fig. 8(b) and (d), these two controllers can obviously achieve the improvements in the vertical and pitch angular acceleration. Nevertheless, the proposed QLF-based controller has a smoother acceleration response, which implies that the controller has a better control performance with respect to the BLF-based controller.

Fig. 9 shows the tracking errors of e_1, e_2, e_3 and e_4 for active suspension system with the two controllers under random road excitation. By analyzing Fig. 9, we can obtain that the tracking errors of the QLF-based controller can converge to zero within less time, which demonstrates the proposed controller has the desirable control responses.

4.3. Periodic response

In order to further evaluate the control effect of the proposed controller, by following the same procedure as in Sections 4.1 and 4.2, we give the expression of the classical periodic road excitation for this case, which is written as [39]

$$\begin{aligned} z_r(t) = {} & 0.0254\sin(2\pi t) + 0.005\sin(10.5\pi t) \\ & +0.001\sin(21.5\pi t) \end{aligned} \tag{62}$$

Note that this type of road excitation is simulated by integrating the low frequency vibration response that is close to the vehicle body resonance frequency (1 Hz), and the high frequency vibration response. Similarly, only the time-series comparisons of the vertical displacement and acceleration response for active suspension system with these two different controllers under Case I and Case II conditions, as well as the comparison of tracking errors under non-zero initial condition are provided.

4.3.1. Simulation analysis in Case I

Now we explore the output responses for active suspension system in Case I under the periodic road excitation, and the corresponding time-series curves are shown in Fig. 10. It is obviously concluded from Fig. 10(a) and (c) that, compared to uncontrolled suspension system, both of the BLF-based and QLF-based controllers can effectively isolate vibrations and perturbations caused by the road disturbance. Additionally, according to Fig. 10(b) and (d), it is similar to the situations in bump and random responses that both of the two controllers can significantly improve the vertical and pitch angular acceleration to make the control system converge to a relatively stable state in less time.

4.3.2. Simulation analysis in Case II

We show the time-series of the displacement and acceleration in Fig. 11 for active suspension system with the two controllers in Case II under the periodic road excitation. Like the corresponding simulation results of Case II in bump and random responses, we can observe the similar improvements of suspension performance when using the two adaptive backstepping controllers and the closed-loop control system in (5) converges to a relatively stable state in the presence of periodic signal interference within less time.

Fig. 12 reveals the tracking errors of active suspension system with the two controllers under the periodic road excitation. It is observed from Fig. 12 that the tracking error of QLF-based controller can converge to zero within less time in tracking the vertical displacement and velocity of $e_1(t)$ and $e_3(t)$, the pitch angular displacement and velocity of $e_2(t)$ and $e_4(t)$, respectively, which demonstrates the proposed controller has the desirable control responses.

4.4. Frequency response analysis

According to ISO 2361 criteria, human body is more sensitive to the vertical vibrations in 4–8 Hz. To evaluate the control performance of the proposed adaptive tracking controller in frequency domain, the power spectral density (PSD) comparison of $\ddot{z}_c$ and $\ddot{\phi}$ under bump, random and periodic road excitation are respectively presented in Figs. 13–15 to compare the variation of tracking errors for active suspension system under Case II condition.

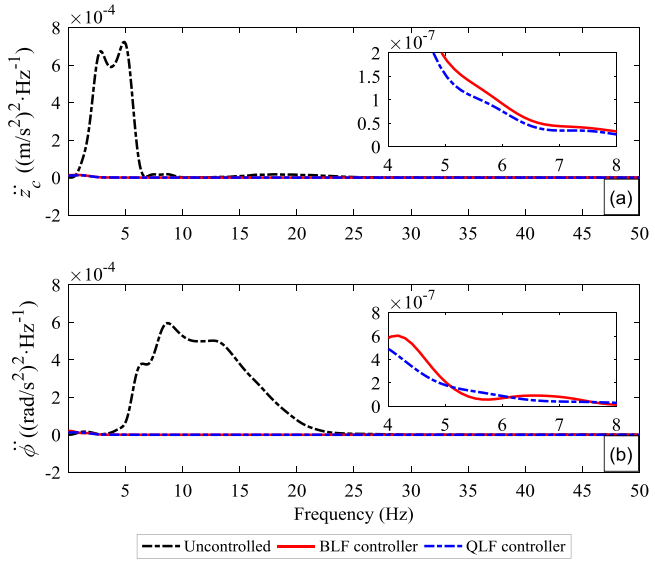

Fig. 13. PSD comparison of (a) vehicle body acceleration, (b) pitch angular acceleration in Case II under bump road.

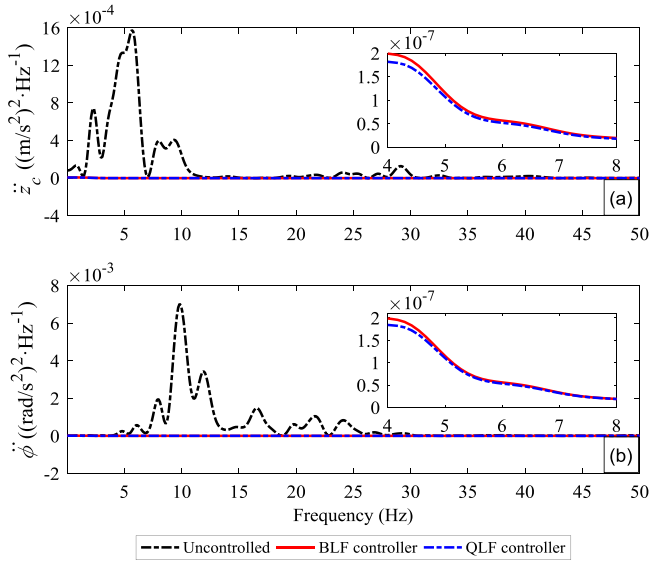

Fig. 14. PSD comparison of (a) vertical acceleration, (b) pitch angular acceleration in Case II under random road.

It can be seen from Figs. 13 to 15 that compared to uncontrolled suspension system, both of the BLF-based and QLF-based controllers can effectively restrain the vertical acceleration and pitch angular acceleration of vehicle body within a certain range, and simultaneously, the proposed QLF-based controller has a lower peak value of vehicle acceleration responses. Finally, Tables 2–4 summarizes the root mean square values (RMS) comparisons of $\ddot{z}_c$ and $\ddot{\phi}$ using different controllers (uncontrolled, BLF and QLF) under Case II in the presence of bump, random and periodic road disturbances, respectively, the calculation expressions of RMS are given by

$$\begin{aligned} \ddot{z}_c(t)_{\mathrm{RMS}} &= \sqrt{\frac{1}{t}\int_0^t (\ddot{z}_c(t))^2 dt} \\ \ddot{\phi}(t)_{\mathrm{RMS}} &= \sqrt{\frac{1}{t}\int_0^t (\ddot{\phi}(t))^2 dt} \end{aligned} \tag{63}$$

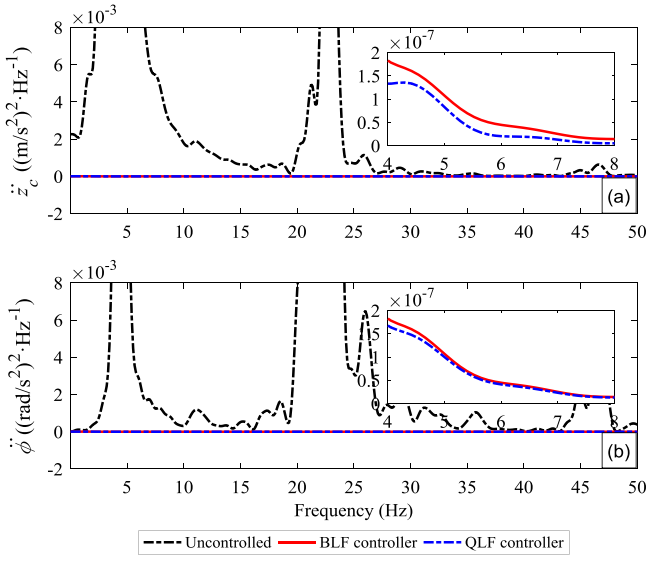

Fig. 15. PSD comparison of (a) vertical acceleration, (b) pitch angular acceleration in Case II under periodic road.

Table 2
RMS comparisons of vehicle body acceleration and pitch angular acceleration under bump road excitation.

Signal	Controller		
($x_1 = 6$ cm, $x_3 = 6$ rad)	Uncontrolled	BLF Controller	QLF Controller
RMS $\ddot{z}_c$	0.4470	0.0605(↓86.47%)	0.0540(↓87.91%)
RMS $\ddot{\phi}$	1.1670	0.0616(↓94.72%)	0.0564(↓95.17%)

Table 3
RMS comparisons of vehicle body acceleration and pitch angular acceleration under random road excitation.

Signal	Controller		
($x_1 = 6$ cm, $x_3 = 6$ rad)	Uncontrolled	BLF Controller	QLF Controller
RMS $\ddot{z}_c$	0.3649	0.0559(↓84.68%)	0.0538(↓85.26%)
RMS $\ddot{\phi}$	1.0408	0.0569(↓94.53%)	0.0553(↓94.69%)

Table 4
RMS comparisons of vehicle body acceleration and pitch angular acceleration under periodic road excitation.

Signal	Controller		
($x_1 = 6$ cm, $x_3 = 6$ rad)	Uncontrolled	BLF Controller	QLF Controller
RMS $\ddot{z}_c$	0.9184	0.0545(↓94.07%)	0.0375(↓95.92%)
RMS $\ddot{\phi}$	1.2807	0.0556(↓95.66%)	0.0538(↓95.80%)

As shown in Table 2, compared to uncontrolled suspension system, the RMS values of $\ddot{z}_c$ and $\ddot{\phi}$ for the BLF-based and QLF-based controller can be enhanced about 86.47%, 87.91% and 94.72%, 95.17%, respectively, under bump road excitation. Next, from Table 3, the RMS values of $\ddot{z}_c$ and $\ddot{\phi}$ for the BLF-based and QLF-based controller can also be enhanced about 84.68%, 85.26% and 94.53%, 94.69%, respectively, under C-class random road excitation. Moreover, it is concluded from Table 4 that the RMS values of $\ddot{z}_c$ and $\ddot{\phi}$ for the BLF-based and QLF-based controller can be greatly enhanced about 94.07%, 95.92% and 95.66%, 95.80%, respectively, under periodic road excitation. This shows that the proposed QLF-based controller can improve vehicle ride quality while satisfying the safety performance constraints under different road profiles, which further illustrates that the designed controller has better control performances.

5. Conclusions

In this paper, an enhanced adaptive backstepping-based tracking controller for nonlinear active suspension system has been proposed with considering the parameters uncertainties, safety performance constraints and external road disturbances, simultaneously. By introducing the virtual control inputs and reference trajectories, the adaptive control law is developed to stabilize both of the vertical and pitch motions of vehicle body by using backstepping technique and Lyapunov stability theory, and further to track the predefined reference trajectories within a finite time. Next, the stability analysis on zero dynamics system is conducted to ensure that the safety performance signals are all bounded and their upper bounds are estimable. Finally, a numerical simulation is provided to demonstrate the effectiveness and validity of the proposed controller through addressing the comparability between the BLF-based adaptive controller and the proposed QLF-based controller. The simulation results show that both of the adaptive backstepping-based controllers can stabilize the vertical and pitch angular in a finite time under zero initial condition, while in non-zero initial condition, the proposed QLF-based controller can achieve greater improvements in ride comfort and safety performance constraints compared with the BLF-based controller. It is worth noticing that, since the safety performance indicators of the control plant has a strong relationship with the preset time of the reference trajectories, how to choose a suitable preassigned time and then archiving the optimized control effect is needed to study in the future.

Acknowledgments

This work is supported by National Natural Science Foundation of China under Grant 51675423 and 51305342, and Primary Research & Development Plan of Shannxi Province, China under Grant 2017GY-029.

Conflict of interest

The authors of this paper declare that they have no conflict of interest.

References

[1] Sakthivel R, Santra S, Mathiyalagan K, Selvi S. Robust reliable control for uncertain vehicle suspension systems with input delays. J Dyn Syst Trans ASME 2015;137(4):041003.
[2] Cao D, Song X, Ahmadian M. Editors' perspectives: road vehicle suspension design, dynamics, and control. Veh Syst Dyn 2011;49(1–2):3–28.
[3] Jin Y, Luo X. Stochastic optimal active control of a half-car nonlinear suspension under random road excitation. Nonlinear Dyn 2013;72(1–2):185–95.
[4] Lian RJ. Enhanced adaptive self-organizing fuzzy sliding-mode controller for active suspension systems. IEEE Trans Ind Electron 2013;60(3):958–68.
[5] Li H, Liu H, Gao H, Shi P. Reliable fuzzy control for active suspension systems with actuator delay and fault. IEEE Trans Fuzzy Syst 2012;20(2):342–57.
[6] Sande TPJVD, Gysen BLJ, Besselink IJM, Paulidesb JJH, Lomonovab EA, Nijmeijera H. Robust control of an electromagnetic active suspension system: Simulations and measurements. Mechatronics 2013;23(2):204–12.
[7] Dangor M, Dahunsi OA, Pedro JO, Ali MM. Evolutionary algorithm-based PID controller tuning for nonlinear quarter-car electrohydraulic vehicle suspensions. Nonlinear Dyn 2014;78(4):2795–810.
[8] Sun W, Gao H, Kaynak O. Finite frequency H_∞ control for vehicle active suspension systems. IEEE Trans Control Syst Technol 2011;19(2):416–22.
[9] Sun W, Li J, Zhao Y, Gao H. Vibration control for active seat suspension systems via dynamic output feedback with limited frequency characteristic. Mechatronics 2011;21(1):250–60.
[10] Hayakawa K, Matsumoto K, Yamashita M. Robust H_∞ output feedback control of decoupled automobile active suspension systems. IEEE Trans Automat Control 1999;44(2):392–6.
[11] Lin FJ, Teng LT, Sheh PH. Intelligent adaptive backstepping control system for magnetic levitation apparatus. IEEE Trans Magn 2007;43(5):2009–18.
[12] Zhou J, Wen C, Zhang C. Adaptive backstepping control of uncertain chaotic systems. In: Proc IEEE int conf control and automation, Vol. 372. 2007, p. 2749–54, 6.
[13] Zhou J, Wen C, Yang G. Adaptive backstepping stabilization of nonlinear uncertain systems with quantized input signal. IEEE Trans Automat Control 2014;59(2):460–4.
[14] Wang T, Zhang Y, Qiu J, Gao H. Adaptive fuzzy backstepping control for a class of nonlinear systems with sampled and delayed measurements. IEEE Trans Fuzzy Syst 2015;23(2):302–12.
[15] Zhu ZC, Li X, Shen G, et al. Wire rope tension control of hoisting systems using a robust nonlinear adaptive backstepping control scheme. ISA Trans 2018;72:256–72.
[16] Ye La, Zong Q, Tian B, Zhang X, Wang F. Control-oriented modeling and adaptive backstepping control for a nonminimum phase hypersonic vehicle. ISA Trans 2017;70:161–72.
[17] Yue F, Li X. Robust adaptive integral backstepping control for opto-electronic tracking system based on modified LuGre friction model. ISA Trans 2018;80:312–21.
[18] Zapateiro M, Pozo F, Karimi JM, Hamid R, Karimi Luo N. Landing gear suspension control through adaptive backstepping techniques with H_∞ performance. In: Proc. The 18th IFAC world congr, Vol. 44. Milano; 2011, p. 4809–14, 1.
[19] Li R, Jiao X. Adaptive control with disturbance attenuation for hydraulic active suspension system. Int J Model Identif Control 2012;17(1):78–84.
[20] Nguyen TT, Bui TH, Tran TP, et al. A hybrid control of active suspension system using H_∞ and nonlinear adaptive controls. In: Proc IEEE int symp ind electron, Vol. 2. 2001, p. 839–44, 2.
[21] Ahn KK, Nam DNC, Jin M. Adaptive backstepping control of an electrohydraulic actuator. IEEE Trans Mechatron 2013;19(3):987–95.
[22] Tee KP, Ge SS, Tay EH. Barrier Lyapunov functions for the control of output-constrained nonlinear systems. Automatica 2009;45(1):449–55.
[23] Chen M, Ge S, Ren B. Adaptive tracking control of uncertain MIMO nonlinear systems with input constraints. Automatica 2011;47(3):452–65.
[24] Liu YJ, Tong S, Chen CLP, Li DJ. Adaptive NN control using integral barrier Lyapunov functionals for uncertain nonlinear block-triangular constraint systems. IEEE Trans Cybern 2017;99:1–11.
[25] Li DP, Li DJ. Adaptive neural tracking control for nonlinear time-delay systems with full state constraints. IEEE Trans Syst Man Cybern 2017;47(7):1590–601.
[26] Goyal A, Kumar J, Kumar V. Comparative study of BLF and QLF based backstepping controllers for active suspension system. In: Proc. 39th national systems conference. IEEE; 2016.
[27] Ren B, Ge SS, Tee KP, Lee TH. Adaptive control for parametric output feedback systems with output constraint. In: Proc. 48th IEEE conf. decision and control. 2009, p. 6650–5.
[28] Yagiz N, Hacioglu Y. Backstepping control of a vehicle with active suspensions. Control Eng Pract 2008;16(12):1457–67.
[29] Kalaivani R, Lakshmi P. Adaptive backstepping controller for a vehicle active suspension system. In: IET intl conf on sustainable energy and intelligent system. IET; 2015, p. 152–8.
[30] Sun W, Pan H, Gao H. Filter-based adaptive vibration control for active vehicle suspensions with electrohydraulic actuators. IEEE Trans Veh Technol 2016;65(6):4619–26.
[31] Elbeheiry EM, Kamopp DC, Elaraby ME. Advanced ground vehicle suspension systems - a classified bibliography. Veh Syst Dyn 1995;24(3):231–58.
[32] Li H, Jing X, Karimi HR. Output-feedback based H_∞ control for vehicle suspension systems with control delay. IEEE Trans Ind Electron 2014;61(1):436–46.
[33] Sun W, Pan H, Zhang Y, Gao H. Multi-objective control for uncertain nonlinear active suspension systems. Mechatronics 2014;24(4):318–27.
[34] Yao B, Bu F, Reedy J, Chiu TC. Adaptive robust motion control of single-rod hydraulic actuators: theory and experiments. IEEE Trans Mechatron 2002;5(1):79–91.
[35] Yao B, Xu L. Output feedback adaptive robust control of uncertain linear systems with disturbances. ASME J Dyn Syst Meas Control 2006;128(4):1–9.
[36] Sun M. A barbalat-like lemma with its application to learning control. IEEE Trans Automat Control 2009;54(9):2222–5.
[37] Sun W, Gao HJ, Yao B. Adaptive robust vibration control of full-car active suspensions with electro-hydraulic actuators. IEEE Trans Control Syst Tech 2013;21(6):2417–22.
[38] Sun W, Zhao Z, Gao H. Saturated adaptive robust control for active suspension systems. IEEE Trans Ind Electron 2013;60(9):3889–96.
[39] Du H, Zhang N. Fuzzy control for nonlinear uncertain electrohydraulic active suspensions with input constraint. IEEE Trans Fuzzy Syst 2009;17:343–56.